scientific reports

OPEN

Darcy–Forchheimer couple stress hybrid nanofluids flow with variable fluid properties

Anwar Saeed[1], Poom Kumam[1,2]✉, Taza Gul[3], Wajdi Alghamdi[4], Wiyada Kumam[5] & Amir Khan[6]

The current study provides a detailed analysis of steady two-dimensional incompressible and electrically conducting magnetohydrodynamic flow of a couple stress hybrid nanofluid under the influence of Darcy–Forchheimer, viscous dissipation, joule heating, heat generation, chemical reaction, and variable viscosity. The system of partial differential equations of the current model (equation of motion, energy, and concentration) is converted into a system of ordinary differential equations by adopting the suitable similarity practice. Analytically, homotopy analysis method (HAM) is employed to solve the obtained set of equations. The impact of permeability, couple-stress and magnetic parameters on axial velocity, mean critical reflux condition and mean velocity on the channel walls are discussed in details. Computational effects show that the axial mean velocity at the boundary has an inverse relation with couple stress parameter while the permeability parameter has a direct relation with the magnetic parameter and vice versa. The enhancement in the temperature distribution evaluates the pH values and electric conductivity. Therefore, the *SWCNTs* and *MWCNTs* hybrid nanofluids are used in this study for medication purpose.

List of symbols

u and v	Velocity components
x and y	Cartesian coordinates
T	Hybrid nano fluid temperature
b	Stretching rate constant
T_∞	Ambient temperature
M	Magnetic parameter
T_w	Wall temperature
E	Electric field parameter
E_0	Strength of electric field
ρ_{hnf}	Density of hybrid nanofluid
v_{hnf}	Hybrid nanofluid kinematic viscosity
α_{hnf}	Hybrid nanofluid thermal diffusivity
$(\rho c_p)_{hnf}$	Hybrid nanofluid heat capacity
Ec	Eckert number
J	Current density
C_{fx}	Skin friction coefficient
τ_w	Shear stress
B_0	Strength of magnetic field

[1]Center of Excellence in Theoretical and Computational Science (TaCS-CoE), Faculty of Science, King Mongkut's University of Technology Thonburi (KMUTT), 126 Pracha Uthit Rd., Bang Mod, Thung Khru, Bangkok 10140, Thailand. [2]Department of Medical Research, China Medical University Hospital, China Medical University, Taichung 40402, Taiwan. [3]Department of Mathematics, City University of Science and Information Technology, Peshawar 25000, Pakistan. [4]Department of Information Technology, Faculty of Computing and Information Technology, King Abdulaziz University, Jeddah 80261, Saudi Arabia. [5]Applied Mathematics for Science and Engineering Research Unit (AMSERU), Program in Applied Statistics, Department of Mathematics and Computer Science, Faculty of Science and Technology, Rajamangala University of Technology Thanyaburi, Thanyaburi 12110, Pathumthani, Thailand. [6]Department of Mathematics and Statistics, University Of Swat, Khyber Pakhtunkhwa 19200, Pakistan. ✉email: poom.kum@kmutt.ac.th

β	Casson parameter
Nu_x	Nusselt number
Re_x	Reynolds number
$k = MLT^{-1}$	Couple stress parameter
Q_0	Heat flux
F'	Dimensionless velocity
∞	Ambient condition
w	Condition on surface

Nanofluids contain significant application in the study of heat transfer enhancement. Different researchers showed that nanofluids has better heat transfer competence than traditional fluids, that's why traditional fluids can be exchanged with nanofluids. Its higher thermal capability has diverted many researchers towards the study of nanofluids. This thermal conductivity property of nanofluids, distinguishes it from other fluids making it an important product for industrial sector including biomedicine, transportation, electronics, foods and nuclear reactors. The size of these nanoparticles is very small up to (1–100 nm) which enhanced the conductivity of the basic fluids upon addition. The structures of nanoparticles consist of metal oxide, carbide, nitride and carbon tubes (SWCNT-MWCNT) etc. The nanofluid has first introduced by Choi[1], having applications ranging from manufacturing processes to industries. By applying the magnetic impact, the nanofluid with boundary layer flow towards the moving wedges has studied by Nadeem et al.[2]. Saleem et al.[3] deliberated the heat transmission enhancement rate of different-shaped copper nanoparticles on the flat surface. Gul et al.[4] have examined the fluid motion of a liquid film considering Reynolds model for the variable viscosity. The variable viscosity concept was used by the researchers in the blood flow containing nanomaterials. The valuable work of the researchers Huda et al.[5,6], Ijaz et al.[7], and Sheriff et al.[8] related to the blood based nanofluids is more applicable. The CNTs are usually used in the blood for the cancer therapy, drug deliveries, and other important applications to the medication. The Medepalli et al.[9], Benos et al.[10], Yang et al.[11], Alsagri et al.[12] have used the blood based nanofluids for the various applications of medications.

Couple-stress fluids have wide range of applications in the industries as colloidal solutions, cooling processes, polymer fluids extraction etc.[13]. Contributions on the topic of nanofluid flow under different conditions are depicted in the articles[14–18].

The study of electrically conducted incompressible fluid flows is termed as magnetohydrodynamic (MHD). The forces such as fluid's Lorentz force have significant observations like the global magnetic field effects upon the Earth. This type of arena is certainly created with the help of strong Lorentz forces that are mainly present in Earth liquid core. Since the Lorentz forces are less common in our routine life observations that make the concept of magnetohydrodynamics difficult to understand. In present study, the role of Lorentz forces on fluids has established by taking electrically conducted fluid and propulsion of a magnetohydrodynamic ship. In review of[19], this propulsion technique[20] is attractive in several characteristics, as magnetohydrodynamic (MHD) propulsion does not need any movable parts. There are numerous applications of MHD propulsion as far as the high speed ships are concerned for naval submarines[21]. Baumgartl et al.[22] have inspected the evaluation of MHD effects upon time dependent and independent fluid flow. In this work an exterior weak magnetic field has applied to the flow system. A detail analysis[23,24] has carried out with main focus upon the impact of MHD fluid flow using different flow conditions and geometrical view of the flow system. The magnetohydrodynamic propulsion could be created in several techniques. As electro hydrodynamics is the study of electrically conducting ionized particles motions or atoms and their transportations with the neighboring liquids and electric fields. These particles, molecules or atom and liquid transportation process consists of electro-osmosis, electro-kinesis, electro-phoresis and electro rotation fusing metals[25] in nuclear reactor and electric heater. Andersson[26] has originated closed form solution for the incompressible fluid flow over the surface which was stretching. Over an exponential surface, the numerical and analytical solution for the incompressible fluid flow with the exponential jump of temperature has explained by Magyari and keller[27]. Partha et al.[28] have studied the mutual influence of dissipation and convective flow past a stretched surface. The energy transportation and numerical simulation of viscous fluid flow past a stretching sheet has designed by Elbashbeshy[29]. Ellahi et al.[30] have applied HAM method for the investigation of 3D flow of Carreau liquid using magnetic effects. Rashidi et al.[31] have investigated the Burger's model for nanofluid flow under the impact of magnetic effects.

In 1856 the Henry Darcy has investigated the flow of homogeneous fluids through madium, consisting of void spaces or pores (termed as porous medium). The work has carried out for small velosities and low permeable media. Later, Forchheimer[32] has overcome the drowbacks of Darcy work by inserting the square of flow term in flow eqiuation. Muskat[33] has identified the addtional term as 'Forchheimer' for the first time. Afterwards, a number of investigation have been conducted by differnt people using differnt geometries for fluid flow and heat transfer through porus media. Pal and Mondal[34] have discussed the the mixed convection flow past a permeable medium with differnt flow conditions. Ganesh et al.[35] have inspected the nanofluid flow past a shrinkng and stretching porous surface with application of second order slip condition. Seddeek[36] has discussed the combined effects of themophoresis and viscous dissipation for investigation of mixed convective Darcy Forchheimer flow through a permeable surface. It has observed in this study that, the flow has reduced with augmentation in inertia cofficient and porosity parameter. Hayat et al.[37] have used the Cattaneo Christove thermal flux model to Darcy Forchheimer flow with varying heat conductivity through porous surface. A number of viscoelastic models have been developed to explain the properties and behavior of non-Newtonian fluids, including the couple stress fluid model. These fluids' constitutive equations are frequently complicated, including a large number of parameters. The couple stress fluid model is the most simple modification of the classical theory of fluids, allowing for polar effects in the fluid medium such as couple stresses and body couples. A couple stress fluids are used in the
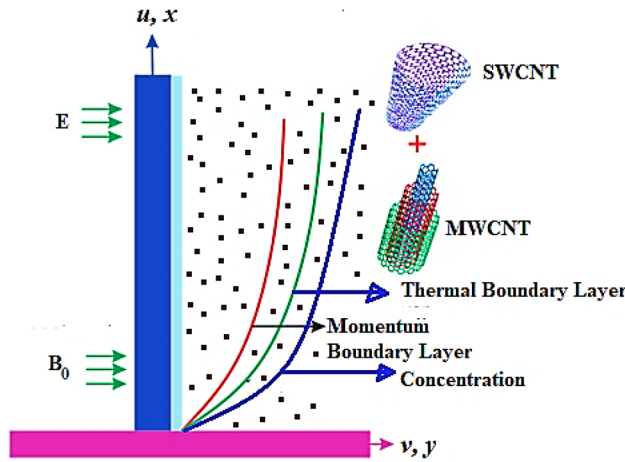
Figure 1. Geometry of the problem.

chemical and engineering sectors. Sinha and Singh[38] investigated the effects of couple stresses on blood flow via a narrow artery with slight stenosis.

In daily life, most of the physical phenomen are non-linear rather some are highly nonlinear phenomenon. Solution of such complex and complicated physical problems is very difficult, even in some cases it becomes impposible to obtaine the analytical solution. In order to solve such problems most of the investigators are emloying different numerical or analytical techniques. Out of such techniques, HAM[39–44] is also useful for solution of such problems.

Principal aim of this research is to inspect the heat transmission and the influence of electro-magnetic effects upon MHD flow of a couple stress hybrid nanofluids over a Darcy-Forchheimer model in a symmetric flow with variable viscosity. The equations investigating the electro-magneto hydrodynamic of MHD flow for a hybrid fluid have converted to non-dimensional notation with suitable variables. The semi-analytical technique HAM is employed to solve the obtained set of equations. The impact of permeability, couple-stress and magnetic parameters on axial velocity, mean critical reflux condition and mean velocity on the channel walls are examined in details. The augmentation in the temperature distribution assesses the pH values and electric conductivity. Consequently, the *SWCNTs* and *MWCNTs* hybrid nanofluids are utilized in this study for medication purpose.

Mathematical modeling

Take a two-dimensional electro-hydrodynamic flow of viscous liquid couple stress nanofluid past a stretching surface. The fluid is stabilized by the collective effects of electric and magnetic fields. The effects of Joule heating and viscous dissipation have also been considered for the current flow system in order to control its thermal characteristics. The mathematical expression for Lorentz force is described as $\vec{J} \times \vec{B}$ in which the magnetic field is represented by $\vec{B}$ while current density by $\vec{J}$. Mathematically the expression for $\vec{J}$ by Ohm's law is described as $\vec{J} = \sigma \left(\vec{E} + \vec{V} \times \vec{B} \right)$. Where 'E' stands for electric field such that $\vec{E} = 0$, while the field electrical conductivity is given by 'σ'. The temperature of nanofluid at surface of wall is T_w, whereas at the free stream it is T_∞. The complete geometry of the current model is shown in Fig. 1.

By applying the above suppositions, resultant equations are:

$$\frac{\partial v}{\partial y} + \frac{\partial u}{\partial x} = 0, \tag{1}$$

$$\rho_{hnf} \left(u \frac{\partial u}{\partial x} + v \frac{\partial u}{\partial y} \right) = \frac{\partial}{\partial y} \left(\mu_{hnf}(T) \frac{\partial u}{\partial y} \right) + \sigma_{hnf} \left(E_0 B_0 - B_0^2 u \right) - \frac{\mu_{hnf}(T)}{K} u - F_0 u^2 - \eta_0 \frac{\partial^4 u}{\partial y^4}, \tag{2}$$

$$(\rho c_p)_{hnf} \left(u \frac{\partial T}{\partial x} + v \frac{\partial T}{\partial y} \right) = k_{hnf} \frac{\partial T^2}{\partial y^2} + \mu_{hnf}(T) \left(\frac{\partial u}{\partial y} \right)^2 + \sigma_{hnf}(uB_0 - E_0)^2 + Q_0(T - T_\infty), \tag{3}$$

$$\left(u \frac{\partial C}{\partial x} + v \frac{\partial C}{\partial y} \right) = D_m \frac{\partial C^2}{\partial y^2} - k_r(C - C_\infty), \tag{4}$$

The subjected conditions at boundary are:

$$\begin{aligned} u = \ u_w(x) \ = \ bx, \ v = 0, \ T = T_w, \ C = C_w \ \ at \ \ y = 0, \\ u = 0, \ \ v = 0, \ \ T \to T_\infty, \ \ C \to C_\infty \qquad at \ y \to \infty. \end{aligned} \tag{5}$$

Above u, v are flow components along the x and y coordinate axes, ρ_{hnf} is hybrid nanofluid density, E_0 is the strength of electric field, B_0 strength of magnetic field and $F_0 = \frac{C_b}{\sqrt{K}}$ is Non-uniform inertia coefficient of porous medium. The kinematic viscosity is ν_{hnf}, heat diffusivity is α_{hnf}, heat capacity is $(\rho c_p)_{hnf}$, dynamic viscosity is given by μ_{hnf}, and Q_0 is heat source. C denotes nanoparticle concentration, k_r chemical reaction.

Thermophysical properties. The mathematical expression for thermophysical properties of base and hybrid nanofluid are described as[4–8]:

$$\frac{\mu(T)_{hnf}}{\mu_f} = \frac{1}{(1-\phi_1)^{2.5}(1-\phi_2)^{2.5}}e^{-m(T-T_\infty)} = \frac{\mu_{hnf}}{\mu_f}e^{-m(T-T_\infty)} = \frac{\mu_{hnf}}{\mu_f}e^{\Lambda\Theta},$$

$$\frac{\rho_{hnf}}{\rho_f} = \left[(1-\phi_2)\left\{1-\left(1-\frac{\rho_{MWCNTs}}{\rho_f}\right)\phi_1\right\} + \phi_2\frac{\rho_{SWCNTs}}{\rho_f}\right] \tag{7}$$

$$\frac{k_{hnf}}{k_{bf}} = (1-\phi_2) + 2\phi_2\left(\frac{k_{SWCNT}}{k_{SWCNT}-k_{bf}}\right)ln\left(\frac{k_{SWCNT}+k_{bf}}{2k_{bf}}\right),$$
$$\frac{k_{bf}}{k_f} = (1-\phi_1) + 2\phi_1\left(\frac{k_{MWCNT}}{k_{MWCNT}-k_f}\right)ln\left(\frac{k_{MWCNT}+k_f}{2k_f}\right). \tag{8}$$

$$\frac{(\rho Cp)_{hnf}}{(\rho Cp)_f} = \left[(1-\phi_2)\left\{1-\left(1-\frac{(\rho Cp)_{MWCNTs}}{(\rho Cp)_f}\right)\phi_1\right\} + \phi_2\frac{(\rho Cp)_{SWCNTs}}{(\rho Cp)_f}\right] \tag{9}$$

The following appropriate variables are suggested:

$$u = b\, x\, F'(\eta), \quad v = -\sqrt{b\,\nu}\, F(\eta), \quad \Theta(\eta) = \frac{T-T_\infty}{T_w-T_\infty}, \quad \Phi(\eta) = \frac{C-C_\infty}{C_w-C_\infty}, \quad \eta = y\sqrt{\frac{b}{\nu}}, \tag{10}$$

Using Eq. (10) in Eqs. (1–5) we have

$$F''' + \frac{\rho_{hnf}}{\rho_f}\frac{\mu_f}{\mu_{hnf}}e^{\Lambda\Theta}\left[FF'' - (1+Fr)F'^2\right] + \frac{\mu_f}{\mu_{hnf}}e^{\Lambda\Theta}\left[M(E-F')^2 - kF^v\right] - \lambda F' = 0, \tag{11}$$

$$\frac{k_{hnf}}{k_f}\Theta'' + Pr\frac{(\rho Cp)_{hnf}}{(\rho Cp)_f}F\Theta' + \frac{\mu_{hnf}}{\mu_f}e^{\Lambda\Theta}Ec\,Pr\left(F''^2 + M(E-F')^2\right) + Q\,Pr\,\Theta = 0, \tag{12}$$

$$\Phi'' + ScF\Phi' - \gamma Sc\Phi = 0. \tag{13}$$

With inter-related boundary conditions:

$$F(0) = 0, F'(0) = 1, \Theta(0) = 1, \Phi(0) = 1$$

$$F(\infty) = 0, \Theta(\infty) = 0, \Phi(\infty) = 0. \tag{14}$$

In above equations the dimensionless couple stress parameter is k, the Prandtl number is Pr, M is magnetic parameter, Q is heat flux parameter, E is electric field parameter and Ec is Eckert number. The mathematical descriptions for these parameters are given as follows:

$$E = \frac{E_0}{B_0 u_w}, Fr = \frac{xC_b}{K^{1/2}}, M = \frac{\sigma B_0^2}{b\rho_f}, Ec = \frac{u_w^2}{c_p(T_w-T_\infty)}, Pr = \frac{\nu_f}{\alpha_f}, Q = \frac{Q_0}{b(\rho c_p)_f}. \tag{15}$$

Engineering quantities. The Skin friction, heat and mass fluxes have numerous uses in engineering field. The mathematical expression for these quantities is given as:

$$C_{fx} = \frac{\tau_w}{\frac{1}{2}\rho_{hnf}(u_w)^2}, \quad Nu_x = \frac{xq_w}{k_{hnf}(T_w-T_\infty)}, \quad Sh_x = \frac{xj_w}{D_{hnf}(T_w-T_\infty)}. \tag{16}$$

Incorporating Eq. (10) in Eq. (16) we have

$$C_{fx}Re_x^{0.5} = \frac{2}{(1-\phi_1)^{2.5}(1-\phi_2)^{2.5}}F''(0), \quad Nu_xRe_x^{-0.5} = -\frac{k_{hnf}}{k_f}\Theta'(0), Sh_xRe_x^{-0.5} = -\Phi'(0). \tag{17}$$

Method of solution. To solve Eqs. (11–13) with the help of Eq. (14), the semi-analytical technique HAM has used. This method requires some starting values which are given mathematically as follows:

$$\widehat{F}(\eta) = 1 - e^{-\eta}, \widehat{\Theta}(\eta) = e^{-\eta}, \widehat{\Phi}(\eta) = e^{-\eta}, \tag{18}$$

$$L_{\widehat{F}}(\widehat{F}) = \widehat{f'''}, \quad L_{\widehat{\Theta}}(\widehat{\Theta}) = \widehat{\Theta}'', \quad L_{\widehat{\Phi}}(\widehat{\Phi}) = \widehat{\Phi}'', \tag{19}$$

The operators $L_{\widehat{F}}, \ L_{\widehat{\Theta}}, L_{\widehat{\Phi}}$ are given as

$$L_{\widehat{F}}(e_1 + e_2\eta + e_3\eta^2) = 0, \quad L_{\widehat{\Theta}}(e_4 + e_5\eta) = 0, \quad L_{\widehat{\Phi}}(e_6 + e_7\eta) = 0. \tag{20}$$

The nonlinear operators $N_{\widehat{F}}, \ N_{\widehat{\Theta}}$ and $N_{\widehat{\Phi}}$ are expressed as:

$$N_{\widehat{F}}\left[\widehat{F}(\eta;\zeta)\right] = \widehat{F}_{\eta\eta\eta} + \frac{\rho_{hnf}}{\rho_f}\frac{\mu_f}{\mu_{hnf}}e^{\Lambda\Theta}\left[\widehat{F}\widehat{F}_{\eta\eta} - (1+Fr)\widehat{F}_\eta^2\right]$$
$$+ \frac{\mu_f}{\mu_{hnf}}e^{\Lambda\Theta}\left[M\left(E - \widehat{F}_\eta\right)^2 - k\widehat{F}_{\eta\eta\eta\eta}\right] - \lambda\widehat{F}_\eta, \tag{21}$$

$$N_{\widehat{\Theta}}\left[\widehat{F}(\eta;\zeta), \widehat{\Theta}(\eta;\zeta)\right] = \frac{k_{hnf}}{k_f}\widehat{\Theta}_{\eta\eta} + \Pr\frac{(\rho Cp)_{hnf}}{(\rho Cp)_f}\widehat{F}\widehat{\Theta}_\eta$$
$$+ \frac{\mu_{hnf}}{\mu_f}e^{\Lambda\Theta}Ec\Pr\left(\widehat{F}_{\eta\eta}^2 + M\left(E - \widehat{F}_\eta\right)^2\right) + Q\Pr\widehat{\Theta}, \tag{22}$$

$$N_{\widehat{\Phi}}\left[\widehat{F}(\eta;\zeta), \widehat{\Phi}(\eta;\zeta)\right] = (1-\phi_1)(1-\phi_2)\widehat{\Phi}_{\eta\eta} + Sc\widehat{F}\widehat{\Phi}_\eta - \gamma Sc\widehat{\Phi}, \tag{23}$$

For Eqs. (6 and 7) the 0th-order equations are

$$(1-\zeta)L_{\widehat{F}}\left[\widehat{F}(\eta;\zeta) - \widehat{F}_0(\eta)\right] = p\ \hbar_{\widehat{F}}\ N_{\widehat{F}}\left[\widehat{F}(\eta;\zeta)\right]$$

$$(1-\zeta)L_{\widehat{\Theta}}\left[\widehat{\Theta}(\eta;\zeta) - \widehat{\Theta}_0(\eta)\right] = p\hbar_{\widehat{\Theta}}N_{\widehat{\Theta}}\left[\widehat{F}(\eta;\zeta), \widehat{\Theta}(\eta;\zeta)\right] \tag{25}$$

$$(1-\zeta)L_{\widehat{\Phi}}\left[\widehat{\Phi}(\eta;\zeta) - \widehat{\Phi}_0(\eta)\right] = p\ \hbar_{\widehat{\Phi}}N_{\widehat{\Phi}}\left[\widehat{F}(\eta;\zeta), \widehat{\Phi}(\eta;\zeta)\right] \tag{26}$$

While BCs are

$$\widehat{F}(\eta;\zeta)\Big|_{\eta=0} = 0, \qquad \frac{\partial\widehat{F}(\eta;\zeta)}{\partial\eta}\Big|_{\eta=0} = 1,$$
$$\widehat{\Theta}(\eta;\zeta)\Big|_{\eta=0} = 1, \qquad \widehat{\Phi}(\eta;\zeta)\Big|_{\eta=0} = 1, \tag{27}$$
$$\widehat{F}(\eta;\zeta)\Big|_{\eta=\infty} \to 0, \qquad \widehat{\Theta}(\eta;\zeta)\Big|_{\eta=\infty} \to 0, \quad \widehat{\Phi}(\eta;\zeta)\Big|_{\eta=\infty} \to 0,$$

Moreover, we further have

$$\widehat{F}(\eta;1) = \widehat{F}(\eta), \ \widehat{\Theta}(\eta;1) = \widehat{\Theta}(\eta), \ \widehat{\Phi}(\eta;1) = \widehat{\Phi}(\eta). \tag{28}$$

The Taylor's expansion for $\widehat{F}(\eta;\zeta)$ and $\widehat{\Theta}(\eta;\zeta), \widehat{\Phi}(\eta;\zeta)$ about $\zeta = 0$ are given as follows

$$\widehat{F}(\eta;\zeta) = \widehat{F}_0(\eta) + \sum_{n=1}^\infty \widehat{F}_n(\eta)\ \zeta^n,$$
$$\widehat{\Theta}(\eta;\zeta) = \widehat{\Theta}_0(\eta) + \sum_{n=1}^\infty \widehat{\Theta}_n(\eta)\ \zeta^n, \tag{29}$$
$$\widehat{\Phi}(\eta;\zeta) = \widehat{\Phi}_0(\eta) + \sum_{n=1}^\infty \widehat{\Phi}_n(\eta)\ \zeta^n.$$
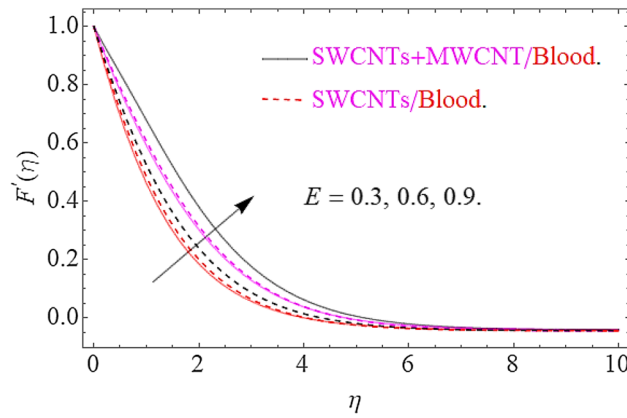
Figure 2. Effects of E on $F'(\eta)$.

$$\widehat{F}_n(\eta) = \frac{1}{n!}\frac{\partial(\eta;\zeta)}{\partial\eta}\bigg|_{p=0}, \widehat{\Theta}_n(\eta) = \frac{1}{n!}\frac{\partial\widehat{\Phi}(\eta;\zeta)}{\partial\eta}\bigg|_{p=0}, \widehat{\Phi}(\eta) = \widehat{\Phi}(\eta) = \frac{1}{n!}\frac{\partial\widehat{\Phi}(\eta;\zeta)}{\partial\eta}\bigg|_{p=0}. \quad (30)$$

While BCs are:

$$\widehat{F}(0) = 0, \ \widehat{F}'(0) = 1, \ \widehat{\Theta}(0) = 1, \ \widehat{\Phi}(0) = 1, \quad (31)$$

$$\widehat{F}'(\eta) \to 0, \ \widehat{\Theta}(\eta) \to 0, \ \widehat{\Phi}(\eta) \to 0, \quad \eta \to \infty. $$

Now

$$\Re_n^{\widehat{F}}(\eta) = \widehat{F}'''_{n-1}$$
$$+ \frac{\rho_{hnf}}{\rho_f}\frac{\mu_f}{\mu_{hnf}}e^{\Lambda\Theta}\left[\sum_{j=0}^{w-1}\widehat{F}_{w-1-j}\widehat{F}''_j - (1+Fr)\widehat{F}'^2_{n-1}\right] + \frac{\mu_f}{\mu_{hnf}}e^{\Lambda\Theta}\left[M\left(E - F'_{n-1}\right)^2 - kF^\nu_{n-1}\right] - \lambda F'_{n-1} = 0, \quad (32)$$

$$\Re_n^{\widehat{\Theta}}(\eta) = \frac{k_{hnf}}{k_f}\widehat{\Theta}''_{n-1} + \Pr\frac{(\rho Cp)_{hnf}}{(\rho Cp)_f}\sum_{j=0}^{w-1}\widehat{F}_{w-1-j}\widehat{\Theta}'_j$$
$$+ \frac{\mu_{hnf}}{\mu_f}e^{\Lambda\widehat{\Theta}}Ec\,\Pr\left(\widehat{F}''^2_{n-1} + M\left(E - \widehat{F}'_{n-1}\right)^2\right) + Q\,\Pr\,\widehat{\Theta}_{n-1} = 0, \quad (33)$$

$$\Re_n^{\widehat{\Phi}}(\eta) = (1-\phi_1)(1-\phi_2)\widehat{\Phi}''_{n-1} + Sc\sum_{j=0}^{w-1}\widehat{F}_{w-1-j}\widehat{\Phi}'_j - \gamma Sc\widehat{\Phi}_{n-1} = 0. \quad (34)$$

While

$$\chi_n = \begin{cases} 0, & \text{if } \zeta \leq 1 \\ 1, & \text{if } \zeta > 1. \end{cases} \quad (35)$$

Discussion of results

In this work we have thoroughly inspected the flow of fluid and transmission of heat for a couple stress nanoliquid inserted among the viscous fluid packed through a horizontal conduit. We shall discuss the impact of different physical factors upon the fluid flow system in following paragraphs with the help of graphical view.

Velocity profile. The influence of different physical parameters such as E, M, λ, F_r, k upon flow field $F'(\eta)$ has presented in Figs. 2, 3, 4, 5 and 6. Figure 2 exposed the effect of electric field on velocity field $F'(\eta)$. In the presence of electrical effects, the field of velocity decreases and at a certain distance away from the wall, it rises closed to the nonlinear stretching sheet. In Fig. 3 we found that, the magnetic effect has reduced the flow field. Actually, for increasing values of M there is a generation of Lorentz force in opposite direction of flow field that declines the velocity filed. This physical phenomenon augments the thermal and concentration characteristics. The effect of porosity parameter λ shows a decrement in the flow profile as depicted in Fig. 4. Physically, for
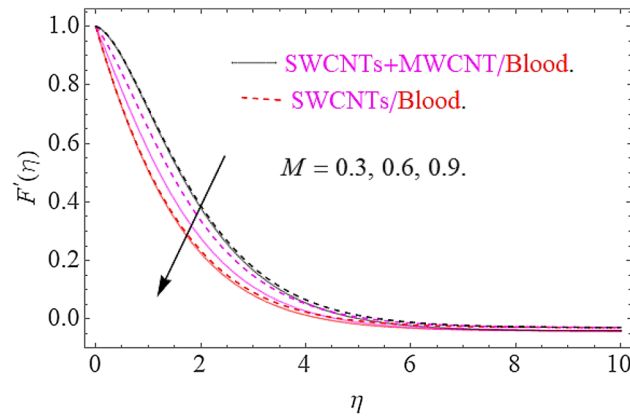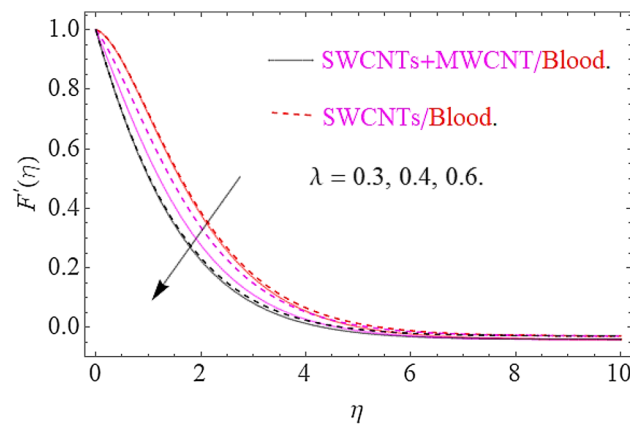
Figure 3. Impact of M on $F'(\eta)$.

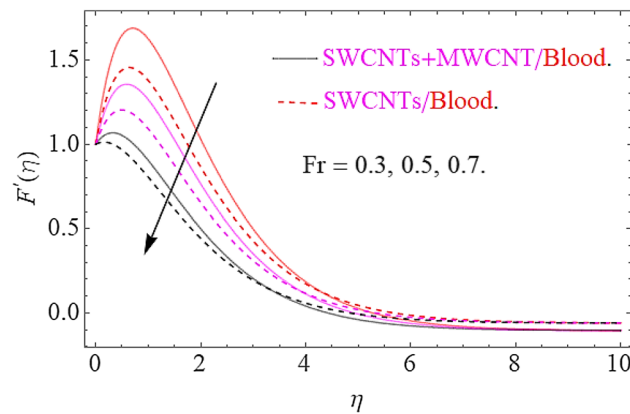**Figure 4.** Impact of λ on $F'(\eta)$.

Figure 5. Influence of Fr on $F'(\eta)$.

increasing values of λ, the void spaces in the medium augments, that offers more resistive force to fluid motion. In this process the flow of fluid declines. Figure 5 depicts the impact upon flow profile for augmentation in inertia coefficient F_r. From this figure, it has perceived that an augmentation in F_r results in generation of resistive force to fluid motion, that result a reduction in flow profile. Figure 6 calculates the influence of k upon flow profile. It has revealed from this figure that, for augmenting values of k the viscous forces will jump up that acts as a reducing agent to fluid motion. Hence the flow profile declines for growth in k.
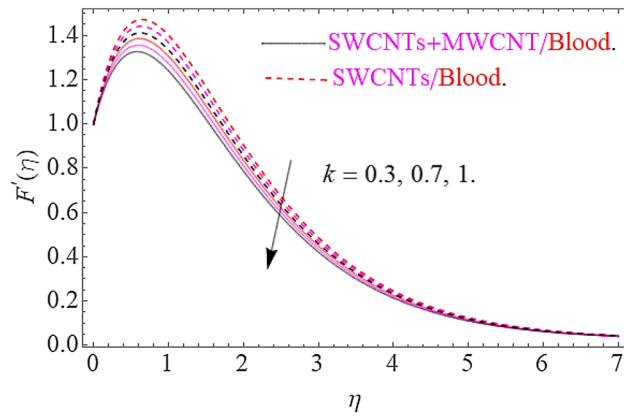
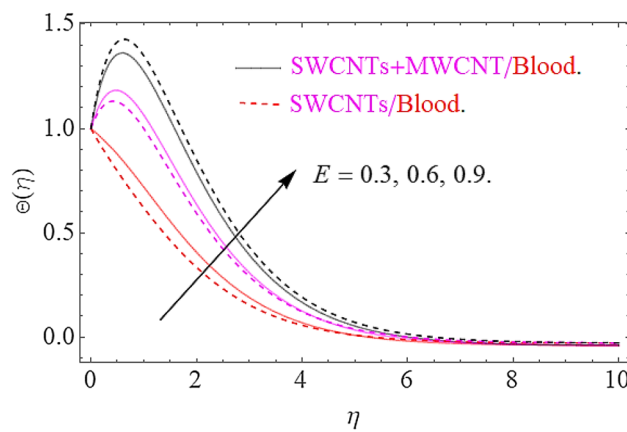**Figure 6.** Effects of k on $F'(\eta)$.

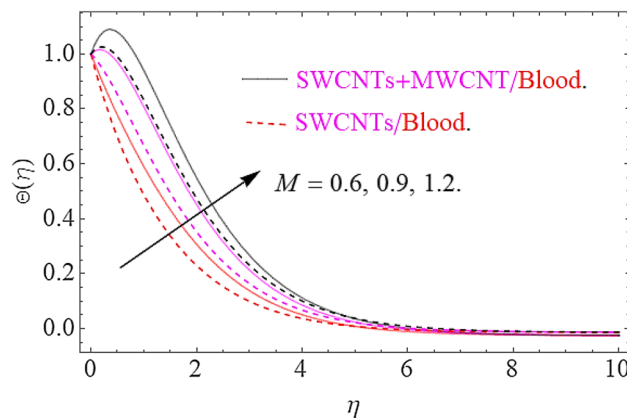**Figure 7.** Impact of E on $\Theta(\eta)$.

Figure 8. effects of M on $\Theta(\eta)$.

Thermal profile. Impact of substantial parameters $Pr, E, M, Ec, \phi_1 = \phi_2$ on temperature variation $\theta(\eta)$ is shown in Figs. 7, 8, 9 and 10. The effects of electric filed E depict in Fig. 7. Clearly the electric filed is directly proportional to the rise in temperature. Hence increase in E accelerates the Lorentz force due to which temperature of nanoparticles increases. Figure 8 depicts that hike in magnetic parameter corresponds to an augmentation in temperature profile. Physically, higher values of M pushes the Lorentz force that creates a resistance to the fluid motion. In this phenomenon the thermal profile jumps up. The increase in Eckert number Ec causes an augmentation in thermal flow as portrays in Fig. 9. Actually, due to higher values of Ec the fluid friction amongst nano-
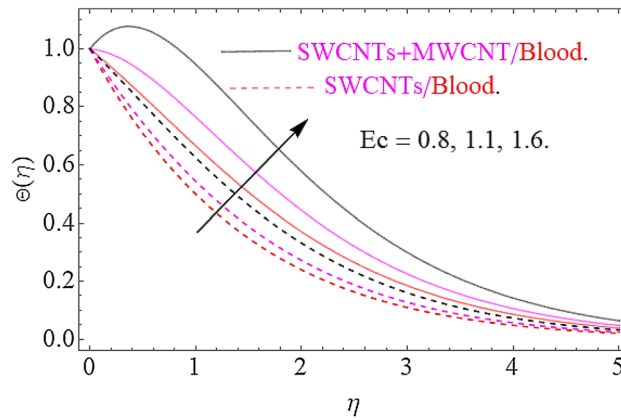
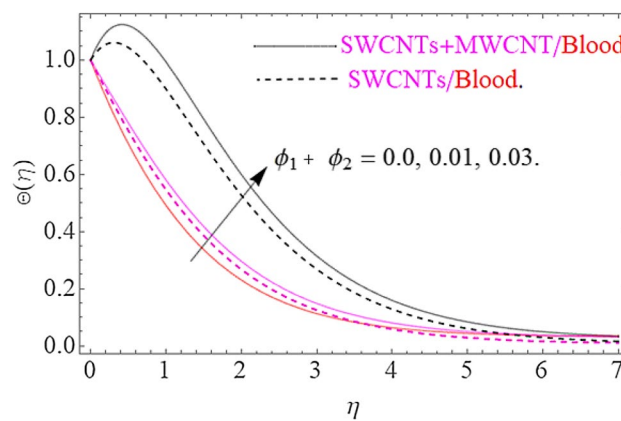**Figure 9.** Impact of Ec on $\Theta(\eta)$.

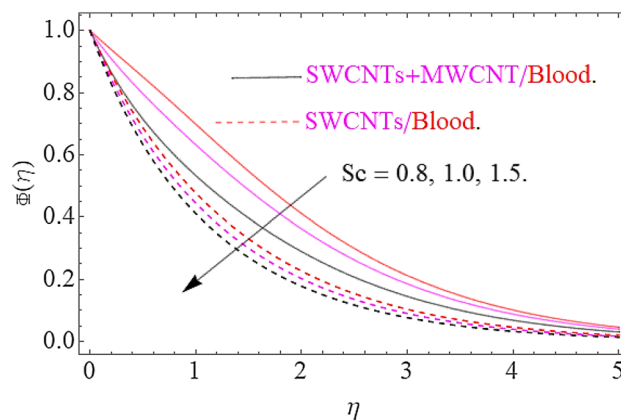**Figure 10.** Effects of $\phi_1 = \phi_2$ on $\Theta(\eta)$.

Figure 11. Impact of Sc on $\Phi(\eta)$.

particles generates with more intensity. In this physical phenomenon the kinetic energy transformed to thermal energy that finally supports the augmentation in thermal profile. Similarly, augmenting values of volumetric friction causes increase in the dense behavior of the fluid particles. In this physical procedure the flow of fluid depreciates and thermal behavior of fluid particles appreciates. Hence the higher values of $\phi_1 = \phi_2$ corresponds to augmentation in thermal profile as depicted in Fig. 10.

Concentration profiles. The result of physical parameters Sc, γ, $\phi_1 = \phi_2$ has been observed for concentration distribution $\phi(\eta)$ in Figs. 11, 12 and 13. Influence of Schmidt number upon dimensionless concentration
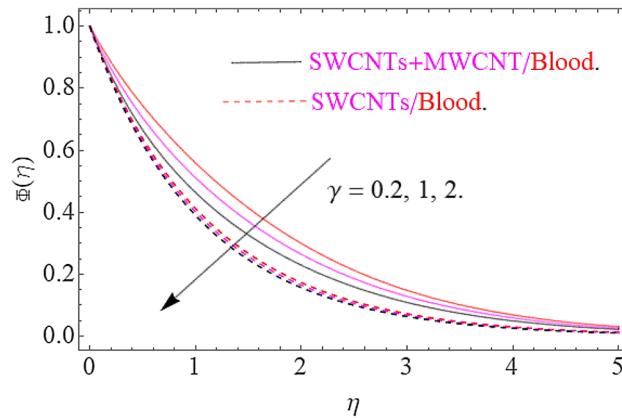
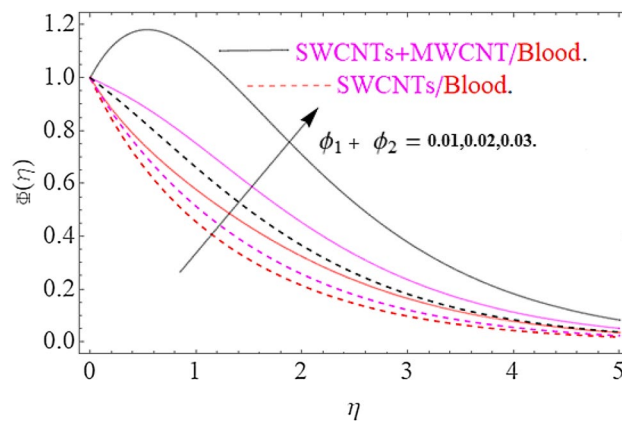**Figure 12.** Influence of γ on $\Phi(\eta)$.

Figure 13. Impact of $\phi_1 = \phi_2$ on $\Phi(\eta)$.

profile is displayed through Fig. 11. This figure illustrates that an upsurge in Schmidt number with respect to a weaker solute diffusion allows a deep penetration of solutal effect. As a result, the concentration decreases with increase in Sc. Figure 12 depicts that, rising in the chemical reaction parameter rapidly reduces the concentration profile. The major reason is that, the number of molecules of solute involved a chemical reaction increase with rise in chemical reaction parameter, which results in decrease of concentration field. Moreover, it is verified that the concentration of profile becomes sharp for augmentation in chemical reaction. The Fig. 13 clearly shows the effects of volume friction upon concentration. Physically, the thermal conductivity increases by boosting the volume concentration of nanoparticles and as a result the nanoparticles act as bridge to pass the heat flow. In this physical phenomenon the concentration profile jumps up as depicted in Fig. 13.

Tables discussion. The physical parameters influenced on the drag force for the nanofluid and hybrid nanofluid have been demonstrated in Table 1. The higher magnitude of parameters $\phi_1 + \phi_2, \Lambda, M, k, Fr, \lambda$ increasing the skin friction coefficient and these consequences are relatively larger in the hybrid nanofluids. The electric field parameter declines the drag force for its increasing value and very small difference between the traditional and hybrid nanofluids has obtained. The rate of heat transfer for nanofluid and hybrid nanofluid versus different parameters has been displayed in Table 2. The augmentation in $\phi_1 + \phi_2, M, Q, Ec$ is enhancing the rate of thermal transmission while the increasing value for viscosity parameter Λ declines this physical quantity. The characteristics of the Schmitt number Sc, chemical reaction parameter γ and nanoparticle volume fraction ϕ_1, ϕ_2 are displayed in Table 3. It has been revealed that greater values of these parameters have augmented the concentration rate.

Conclusions

Health acquired infections (IACs) is a main public health issue worldwide. Whereas CNTs nanofluid plays its important role as antimicrobial. Carbon properties have a strong antimicrobial perspective and CNTs nanofluids are used in the Escherichia coli culture to assess their antibacterial potential. The improvement in the temperature distribution appraises the pH values and electric conductivity. Thus, the *SWCNTs* and *MWCNTs* hybrid nanofluids are used in this study for medication purpose.

Λ	k	$\phi_1 + \phi_2$	M	E	Fr	λ	SWCNTs − Cf_x	SWCNTs + MWCNTs − Cf_x
0.2	0.1	0.01	0.2	0.2	0.2	0.2	1.01150	1.023411
0.4							1.12242	1.13451
0.5							1.23231	1.243442
	0.3						1.24024	1.264234
	0.5						1.26103	1.2832161
		0.02					1.22342	1.2343212
		0.03					1.32512	1.336242
			0.4				1.431272	1.442461
			0.6				1.4423625	1.4535219
				0.4			1.4364210	1.42432041
				0.6			1.422154	1.4103210
					0.4		1.55721321	1.568231023
					0.6		1.56762421	1.57882314
						0.4	1.6320142	1.643102101
						0.6	1.7123210	1.72322372

Table 1. Skin friction $C_{fx}Re_x^{0.5}$ for different parameters regarding blood-based hybrid nanofluid.

$\phi_1 + \phi_2$	Λ	M	Q	Ec	SWCNTs − Nu_x	SWCNTs + MWCNTs − Nu_x
0.0	0.2	0.2	0.2	0.2	0.23414214	0.23414214
0.01					0.23625325	0.23956436
0.02					0.238436435	0.242675477
0.03					0.2401023532	0.245786587
	0.4				0.214120101	0.225221312
	0.6				0.2011071123	0.213219021
		0.4			0.3243123021	0.3354210312
		0.6			0.3363201293	0.34643120321
			0.4		0.34632115321	0.35743204310
			0.6		0.3539076321	0.36432109723
				0.4	0.41032034210	0.42370128301
				0.6	0.44532104320	0.45632107341

Table 2. Nusselt number $Nu_xRe_x^{-0.5}$ versus various parameters for Blood-based hybrid nanofluid.

$\phi_1 + \phi_2$	Sc	γ	SWCNTs − Sh_x	SWCNTs + MWCNTs − Sh_x
0.0	0.1	0.1	0.743308321	0.75321401
0.02			0.754219023	0.76320132
0.04			0.764320121	0.77543109
	0.3		0.823457012	0.83421089
	0.5		0.9310764351	0.94219082
		0.3	0.9457832101	0.956704231
		0.5	0.9533442156	0.962245713

Table 3. Sherwood number versus the embedded parameters.

The core purpose of this research is to inspect the heat transfer and the effect of electro-magnetic field upon flow of a couple stress hybrid nanofluid over a Darcy-Forchheimer model in a symmetric flow with variable viscosity. Analytically, HAM is employed to solve the obtained set of equations in non-dimensional arrangement. The impact of encountered parameters has also discussed in detail. During this deep discussion, the underlined points have been revealed:

- In the presence of electric effects, the field of velocity decreases and at a certain distance away from the wall, it rises closed to the nonlinear stretching sheet.

- For increasing values of magnetic effect, there is a generation of Lorentz force in opposite direction of flow field that declines the velocity filed.
- For increasing values of porosity parameter the void spaces in the medium augments that offers more resistance to the flow of fluid and declines the flow profile.
- Augmentation in inertia coefficient results in generation of resistive force to fluid motion that causes a reduction in flow profile.
- For augmentation in Prandtl number the thermal diffusion reduces due to which less heat transfer takes place that ultimately declines the thermal profile.
- An increase in electric field accelerates the Lorentz force due to which temperature of nanoparticles increases.
- Augmentation in magnetic parameter corresponds to an augmentation in temperature profile.
- For higher values of Eckert number, the fluid friction amongst nanoparticles generates with more intensity. In this physical phenomenon the kinetic energy transformed to thermal energy that finally supports the augmentation in thermal profile.
- Augmenting values of volumetric friction causes increase in the dense behaviour of the fluid particles that depreciates the fluid flow and appreciates the thermal behaviour of fluid particles. Moreover, the concentration of fluid also rises in this phenomenon.
- An upsurge in Schmidt number results a reduction in concentration profile.
- Rising values in the chemical reaction parameter rapidly reduces the concentration profile.

References

1. Choi, S.U.S., & Eastman, J.A. *Enhancing Thermal Conductivity of Fluids with Nanoparticles. No. ANL/MSD/CP-84938; CONF-951135-29.* (Argonne National Lab, 1995).
2. Nadeem, S., Ahmad, A. & Muhammad, N. Computational study of Falkner-Skan problem for a static and moving wedge. *Sens. Actuators B Chem.* **263**, 69–76 (2018).
3. Saleem, S., Qasim, M., Alderremy, A. & Noreen, S. Heat transfermenhancement using different shapes of Cu nanoparticles in themflow of water based nanofluid. *Phys. Scr.* **95**, 055209 (2020).
4. Gul, T., Islam, S., Shah, R. A., Khan, I. & Shafie, S. Thin film flow in MHD third grade fluid on a vertical belt with temperature dependent viscosity. *PLoS ONE* **9**(6), e97552. https://doi.org/10.1371/journal.pone.0097552 (2014).
5. Huda, A. B., Akbar, N. S., Beg, O. A. & Khan, M. Y. Dynamics of variable-viscosity nanofluid flow with heat transfer in a flexible vertical tube under propagating waves. *Results Phys.* **7**, 413–425 (2017).
6. Huda, A. B. & Akbar, N. S. Heat transfer analysis with temperature-dependent viscosity for the peristaltic flow of nano fluid with shape factor over heated tube. *Int. J. Hydrogen Energy* **42**(39), 25088–25101 (2017).
7. Ijaz, S., Shahzadi, I., Nadeem, S. & Saleem, A. A clot model examination: With impulsion of nanoparticles under influence of variable viscosity and slip effects. *Commun. Theor. Phys.* **68**(5), 667 (2017).
8. Sheriff, S., Sadaf, H., Akbar, N. S. & Mir, N. A. Slip analysis with thermally developed peristaltic motion of nanoparticles under the influence of variable viscosity in vertical configuration. *Eur. Phys. J. Plus* **134**(8), 408 (2019).
9. Medepalli, K., Alphenaar, B., Raj, A. & Sethu, P. Evaluation of the direct and indirect response of blood leukocytes to carbon nanotubes (CNTs). *Nanomed. Nanotechnol. Biol. Med.* **7**(6), 983–991 (2011).
10. Benos, L., Spyrou, L. A. & Sarris, I. E. Development of a new theoretical model for blood-CNTs effective thermal conductivity pertaining to hyperthermia therapy of glioblastoma multiform. *Comput. Methods Programs Biomed.* **172**, 79–85 (2019).
11. Yang, X. Y. *et al.* Blood-capillary-inspired, free-standing, flexible, and low-cost super-hydrophobic N-CNTs@ SS cathodes for high-capacity, high-rate, and stable Li-air batteries. *Adv. Energy Mater.* **8**(12), 1702242 (2018).
12. Alsagri, A. S. *et al.* MHD thin film flow and thermal analysis of blood with CNTs nanofluid. *Coatings* **9**(3), 175 (2019).
13. Baslem, A. *et al.* Analysis of thermal behavior of a porous fin fully wetted with nanofluids: convection and radiation. *J. Mol. Liq.* **307**, 112920 (2020).
14. Saeed, A. *et al.* Blood based hybrid nanofluid flow together with electromagnetic field and couple stresses. *Sci. Rep.* **11**(1), 1–18 (2021).
15. Gul, T. *et al.* Irreversibility analysis of the couple stress hybrid nanofluid flow under the effect of electromagnetic field. *Int. J. Numer. Methods Heat Fluid Flow* https://doi.org/10.1108/HFF-11-2020-0745 (2021).
16. Gul, T. *et al.* Mixed convection stagnation point flow of the blood based hybrid nanofluid around a rotating sphere. *Sci. Rep.* **11**, 7460 (2021).
17. Alam, M. W. *et al.* CPU heat sink cooling by triangular shape micro-pin-fin: Numerical study. *Int. Commun. Heat Mass Transf.* **112**, 104455 (2020).
18. Kumar, K. G. *et al.* Significance of Arrhenius activation energy in flow and heat transfer of tangent hyperbolic fluid with zero mass flux condition. *Microsyst. Technol.* **26**(8), 2517–2526 (2020).
19. Weier, T., Shatrov, V., & Gerbeth, G. Flow control and propulsion in poor conductors. in *Magnetohydrodynamics*. 295–312 (Springer, 2007).
20. Phillips, O. M. The prospects for magnetohydrodynamic ship propulsion. *J. Ship Res.* **43**, 43–51 (1962).
21. Way, S. Electromagnetic propulsion for cargo submarines. *J. Hydrodyn.* **2**(2), 49–57 (1968).
22. Baumgartl, J., Hubert, A. & Müller, G. The use of magnetohydrodynamic effects to investigate fluid flow in electrically conducting melts. *Phys. Fluids A Fluid Dyn. (1989-1993)* **5**(12), 3280–3289 (1993).
23. Thess, A., Votyakov, E. V. & Kolesnikov, Y. Lorentz force velocimetry. *Phys. Rev. Lett.* **96**(16), 164501 (2006).
24. Priede, J., Buchenau, D. & Gerbeth, G. Contactless electromagnetic phase-shift flow meter for liquid metals. *Meas. Sci. Technol.* **22**(5), 055402 (2011).
25. Woodson, H. H. & Melcher, J. R. *Electromechanical Dynamics* (Massachusetts Institute of Technology, 1968).
26. Andersson, V. P. MHD flow of a viscoelastic fluid past a stretching surface. *Acta Mech.* **95**, 227–230. https://doi.org/10.1007/bf01170814 (1992).
27. Magyari, E. & Keller, B. Heat and mass transfer in the boundary layers on an exponentially stretching continuous surface. *J. Phys. D Appl. Phys.* **32**, 577–585. https://doi.org/10.1088/0022-3727/32/5/012 (1999).
28. Partha, M. K., Murthy, P. V. & Rajasekhar, G. P. Effect of viscous dissipation on the mixed convection heat transfer from an exponentially stretching surface. *Heat Mass Transf.* **41**, 360–366. https://doi.org/10.1007/s00231-004-0552-2 (2005).

29. Elbashbeshy, E. M. A. Heat transfer over an exponentially stretching continuous surface with suction. *Arch. Mech.* **53**, 643–651 (2001).
30. Ellahi, R., Bhatti, M. M. & Khalique, C. M. Three-dimensional flow analysis of Carreau fluid model induced by peristaltic wave in the presence of magnetic field. *J. Mol. Liq.* **241**, 1059–1068 (2017).
31. Rashidi, M. M., Yang, Z., Awais, M., Nawaz, M. & Hayat, T. Generalized magnetic field effects in Burgers' nanofluid model. *PLoS ONE* **12**, 168923 (2017).
32. Forchheimer, P. Wasserbewegung durch boden. *Z. Vereins Deutscher Ingenieure* **45**, 1782–1788 (1901).
33. Muskat, M. The flow of homogeneous fluids through porous media. *Edwards Ann Arbor Michi.* **191**, 6 (1946).
34. Pal, D. & Mondal, H. Hydromagnetic convective diffusion of species in Darcy-Forchheimer porous medium with non-uniform heat source/sink and variable viscosity. *Int. Commun. Heat Mass Transf.* **39**(7), 913–917 (2012).
35. Ganesh, N. V., Hakeem, A. K. A. & Ganga, B. Darcy-Forchheimer flow of hydromagnetic nanofluid over a stretching/shrinking sheet in a thermally stratified porous medium with second order slip, viscous and Ohmic dissipations effects. *Ain Shams Eng. J.* **9**, 939–951 (2016).
36. Seddeek, M. A. Influence of viscous dissipation and thermophoresis on Darcy-Forchheimer mixed convection in a fluid saturated porous media. *J. Colloid Interface Sci.* **293**, 137–142 (2006).
37. Hayat, T., Muhammad, T., Al-Mezal, S. & Liao, S. J. Darcy-Forchheimer flow with variable thermal conductivity and Cattaneo-Christov heat flux. *Int. J. Numer. Methods Heat Fluid Flow* **26**, 2355–2369 (2016).
38. Sinha, P. & Singh, C. Effects of couple stresses on the blood flow through an artery with mild stenosis. *Biorheology* **21**, 303–315 (1984).
39. Gul, T., Nasir, S. & Islam, I. Effective Prandtl number model influences on the γAl_2O_3–H_2O and γAl_2O_3–$C_2H_6O_2$ nanofluids spray along a stretching cylinder. *Arab. J. Sci. Eng.* **44**, 16 (2018).
40. Palwasha, Z., Khan, N. & Shah, Z. Study of two-dimensional boundary layer thin film fluid flow with variable thermophysical properties in three dimensions space. *AIP Adv.* **8**, 105318 (2018).
41. Zuhra, S., Khan, N. & Shah, Z. Simulation of bioconvection in the suspension of second grade nanofluid containing nanoparticles and gyrotactic microorganisms. *AIP Adv.* **8**, 105210 (2018).
42. Khan, N., Zuhra, S. & Shah, Z. Slip flow of Eyring-Powell nanoliquid film containing graphene nanoparticles. *AIP Adv.* **8**, 115302 (2018).
43. Khan, A. S., Nie, Y. & Shah, Z. Three-dimensional nanofluid flow with heat and mass transfer analysis over a linear stretching surface with convective boundary conditions. *Appl. Sci.* **8**, 2244 (2018).
44. Nasir, S., Islam, S. & Gul, T. Three-dimensional rotating flow of MHD single wall carbon nanotubes over a stretching sheet in presence of thermal radiation. *Appl. Nanosci.* **8**, 1361–1378 (2018).

Acknowledgements

Author contributions

A.S., T.G. and P.K. modeled and solved the problem. T.G. and A.S. wrote the manuscript. A.K., T.G. and W.K. contributed in the numerical computations and plotting the graphical results. W.A., T.G. and P.K. work in the revision of the manuscript. The corresponding author finalized the manuscript after its internal evaluation.

Competing interests

The authors declare no competing interests.

Additional information

Correspondence and requests for materials should be addressed to P.K.

Reprints and permissions information is available at www.nature.com/reprints.

Publisher's note Springer Nature remains neutral with regard to jurisdictional claims in published maps and institutional affiliations.